Aust. J. Phys., 1995, **48**, 125–42

Thermonuclear Reaction Rates for Reactions Leading to $N = 28$ Nuclei

A. J. Morton and D. G. Sargood

School of Physics, University of Melbourne,
Parkville, Vic 3052, Australia.

Abstract

Nuclear reaction cross sections derived from statistical-model calculations have been used in the calculation of thermonuclear reaction rates for 36 nuclei at temperatures that are representative of the interiors of evolving stars and supernovae as nucleosynthesis approaches the production of nuclei with $N = 28$. The statistical-model calculations used optical-model parameters in the particle channels which had been selected to give the best overall agreement between theoretical and experimental cross sections for reactions on stable target nuclei in the mass and energy ranges of importance for the stellar conditions of interest. The optical-model parameters used, and the stellar reaction rates obtained, are tabulated. Comparisons are made between these stellar rates and those from other statistical-model calculations in the literature.

1. Introduction

In the late stages of evolution of a massive star ($M \gtrsim 10M_{\odot}$, where $M_{\odot}$ is the mass of the Sun), including the supernova in which it culminates, the networks of nuclear reactions that occur in the stellar interior are greatly influenced by the existence of the neutron closed shell at $N = 28$. This is because, with closure of the neutron shell, additional neutrons are so loosely bound that they tend to be evaporated by (γ, n) reactions almost as quickly as they are captured, and $N = 28$ corresponds to a kind of barrier which severely impedes the advance of nucleosynthesis to elements of higher mass.

In silicon burning, the final energy-producing nuclear process in the star's history, α-particles, produced by photodisintegration of ^{28}Si and the products thereof, drive a chain of α-particle-induced reactions based on ^{28}Si and leading to formation of ^{45}Sc. Following this, a reaction network which may be broadly characterised by repeated occurrence of the reaction sequence (p, γ), (p, γ), (n, p) takes the nucleosynthesis up to the stage where $N = 28$ (Woosley *et al.* 1973). The two $N = 28$ nuclides initially most fed by this network are ^{52}Cr and ^{53}Mn. Thereafter there is build-up in $N = 28$ nuclei, with the dominant species being ^{54}Fe in the evolutionary hydrostatic burning process and ^{56}Ni in the explosive process of the supernova.

According to the scheme of Howard *et al.* (1972), many neutron-rich isotopes owe their existence to a reaction network initiated by rapid chains of neutron captures on seed nuclei during explosive carbon burning. The seeds are products

0004-9506/95/010125$10.00

of explosive oxygen burning in previous-generation stars. The neutron flux rises so high that neutron capture proceeds until isotopes with $N = 28$ are formed. These include species such as ^{46}Ar and ^{47}K, both of which are then further processed in networks of (p, n), (p, γ) and (n, γ) reactions which lead ultimately to formation of nuclei such as ^{48}Ca, ^{48,49,50}Ti and ^{51}V.

Many of the reactions in the networks of these two burning processes involve unstable target nuclei, and calculations of the nucleosynthesis have depended on the use of theoretical cross sections obtained by means of statistical-model codes. The most reliable calculations reported in the literature are those from the statistical-model code HAUSER*4 (Mann 1976) using the optical-model parameters of Morton *et al.* (1994) for reactions passing through $N = 28$ compound nuclei, and those of Tims *et al.* (1988) for $N \neq 28$ compound nuclei. The combination of HAUSER*4 and these optical-model parameters has led to cross sections in agreement with experiment, almost always to within a factor of 1·5 and always to within a factor of 2, for a wide range of reactions (Scott *et al.* 1991; Tims *et al.* 1993; Hansper *et al.* 1993; Morton *et al.* 1994). We have therefore used this procedure to calculate cross sections for all reactions in the main path of nucleosynthesis leading into the $N = 28$ region, for both the burning processes described above, and have calculated stellar reaction rates from these cross sections.

Table 1. Optical-model parameters (in MeV)

Proton parameters for channel $^A_Z X_N$+p at laboratory energy $E_p = E$

	$N \neq 28$	$N = 28$
V	$54{\cdot}0-0{\cdot}32E+0{\cdot}4Z/A^{\frac{1}{3}}+24{\cdot}0(N-Z)/A$	$72{\cdot}0-0{\cdot}5Z^{\dagger}$
R	$1{\cdot}17A^{\frac{1}{3}}$	$1{\cdot}17A^{\frac{1}{3}}$
a	0·75	0·75
W	6*	$9{\cdot}167-0{\cdot}333Z^{\dagger}$
R'	$1{\cdot}32A^{\frac{1}{3}}$	$1{\cdot}32A^{\frac{1}{3}}$
a'	$0{\cdot}51+0{\cdot}7(N-Z)/A$	$0{\cdot}51+0{\cdot}7(N-Z)/A$

Neutron parameters for channel $^A_Z X_N$+n at laboratory energy $E_n = E$

	$N+1 \neq 28$	$N+1 = 28$
V	$56{\cdot}3-0{\cdot}32E-24{\cdot}0(N-Z)/A$	$86{\cdot}6-1{\cdot}067Z^{\dagger}$
R	$1{\cdot}17A^{\frac{1}{3}}$	$1{\cdot}17A^{\frac{1}{3}}$
a	0·75	0·75
W	4*	$10{\cdot}59-0{\cdot}378Z^{\dagger}$
R'	$1{\cdot}26A^{\frac{1}{3}}$	$1{\cdot}26A^{\frac{1}{3}}$
a'	0·58	0·58

Alpha-particle parameters for channel $^A_Z X_N+\alpha$

	$N+2 \neq 28$	$N+2 = 28$
V	185·0	204†
R	$1{\cdot}4A^{\frac{1}{3}}$	$1{\cdot}4A^{\frac{1}{3}}$
a	0·52	0·52
W	10*	10†
R'	$1{\cdot}4A^{\frac{1}{3}}$	$1{\cdot}4A^{\frac{1}{3}}$
a'	0·52	0·52

* Tims *et al.* (1988). † Morton *et al.* (1994).

2. Calculation of Cross Sections

The default optical-model parameters in the code HAUSER*4 are those of Becchetti and Greenlees (1969) in the proton and neutron channels, and those of McFadden and Satchler (1966) in the α-particle channel. They all refer to Woods–Saxon or derivative Woods–Saxon potential wells. These parameters were based on elastic scattering data at energies well above those of interest in nucleosynthesis and on nuclei of masses in excess of those involved in the nucleosynthesis processes discussed here. The parameters of Morton *et al.* (1994) and Tims *et al.* (1988) are modifications of these default parameters: selected well depths were changed to obtain improved overall agreement with experimental reaction cross section data in the mass and energy ranges appropriate to nucleosynthesis. The parameters used in the calculations of this paper are listed in Table 1. The modified well depths of Morton *et al.* and Tims *et al.* are all identified: the rest are the default parameters of Becchetti and Greenlees, and McFadden and Satchler. In each channel there is a real Woods–Saxon well of depth V (MeV), radius R (fm), and diffuseness a (fm); and an imaginary derivative Woods–Saxon well of depth W (MeV), radius R' (fm), and diffuseness a' (fm).

In the calculation of cross sections, advantage was taken of the option in HAUSER*4 to apply width fluctuation corrections in the particle channels, according to the prescription of Tepel *et al.* (1974).

3. Calculation of Stellar Reaction Rates

Thermonuclear reaction rates were calculated from the cross sections by means of the equation

$$\langle\sigma v\rangle^{\mu} = (8/\pi M)^{\frac{1}{2}}(kT)^{-3/2}\int \sigma(E)\,E\,\exp(-E/kT)\,\mathrm{d}E$$

of Fowler *et al.* (1967), where M and E are the reduced mass and centre-of-mass energy, and the superscript μ indicates that the target is in its μth excited state. In a stellar interior, nuclei are in a thermal distribution of excited states, so the stellar reaction rate is given by

$$\langle\sigma v\rangle^{*} = \frac{\sum_{\mu=0}^{\infty}(2J^{\mu}+1)\exp(-\varepsilon^{\mu}/kT)\,\langle\sigma v\rangle^{\mu}}{\sum_{\mu=0}^{\infty}(2J^{\mu}+1)\exp(-\varepsilon^{\mu}/kT)}\,.$$

In practice, the excitation energy ε^{μ}, spin J^{μ}, and parity π^{μ} of the μth excited state were taken from the literature up to the highest excitation for which the literature values were considered reliable and complete, and were based on a density-of-states formula for higher excitations. The density-of-states formula was that for a Fermi back-shifted gas, and the highest value of μ used corresponded to inclusion of 99% of the target nuclei. In some cases where spectroscopic information was unavailable for a given nucleus, it was possible to deduce 'most likely' ground-state and first-excited-state J^{π} and first-excited-state energy from a study of nuclear systematics. In others, extensive data were available for the mirror nucleus, which were considered to be much more reliable for the nucleus in question than those given by the density-of-states formula.

In taking spectroscopic information from the literature compilations, we rejected levels classified as 'of doubtful existence'. In particular, we rejected the $0\cdot388$ MeV state in ^{48}Sc, which would be important for ^{48}Ca(p, γ), (p, n) if it existed, because the only evidence for its existence is a weak yield observed in measurements on ^{49}Ti(t, α)^{48}Sc and the α-particle peak would have been indistinguishable from that from ^{47}Ti(t, α)^{46}Sc feeding the well documented $1\cdot271$ MeV state in ^{46}Sc, and ^{47}Ti would be an almost certain contaminant in the target.

4. The Special Case of ^{52}Mn

The ground state of ^{52}Mn has $J^{\pi} = 6^{+}$ while the $0\cdot378$ MeV first excited state has $J^{\pi} = 2^{+}$ and $t_{1/2} = 21\cdot1$ min. The published decay schemes of the excited states fall into two distinct groups: cascades involving states with $J \leq 4$, leading to the isomeric $0\cdot378$ MeV state; and cascades involving states with $J \geq 5$, leading to the ground state. Crossovers between these two groups are few and mostly weak. The question therefore arises as to whether ^{52}Mn can achieve a thermal distribution of states on a timescale that is short compared with the timescale of its destruction by nuclear reactions in a stellar interior. In other words, can ^{52}Mn be treated as a single nucleus or must it be treated as two independent nuclei?

Following the procedures of Solomon and Sargood (1978) and Ward and Fowler (1980), we calculated the approach to thermal equilibrium, for a number of different temperatures and different initial conditions, on the assumption that all communication between states was by electromagnetic radiation, with the effects of stimulated emission included. For simplicity, we assumed all nuclei to be initially in the ground state or the isomeric state, in varying proportions. The timescale for destruction by nuclear reactions was determined from statistical-model cross sections for ^{52}Mn(p, γ)^{53}Fe and ^{52}Mn(p, n)^{52}Fe, and free proton densities taken from Bodansky *et al.* (1968). The contributions from competing reactions were negligible. Manganese-52 nuclei initially in the ground state achieved thermal equilibrium with the $J \geq 5$ group to within 10% for every state, on a timescale that is short (by a factor > 100) compared with the timescale for destruction by nuclear reactions, and those initially in the isomeric state achieved equilibrium with the $J \leq 4$ group on a similar timescale. In Fig. 1 we show the results for an initial ratio of 1:1 isomer to ground state, corresponding to the results of statistical-model calculations for population of the $J \leq 4$ and $J \geq 5$ states of ^{52}Mn by way of ^{51}Cr(p, γ)^{52}Mn, the dominant mode of production in the scheme of Woosley *et al.* (1973). Clearly, for $T_9 \leq 4\cdot8$, where T_9 is the temperature in units of 10^9 K, an overall thermal distribution is achieved on a timescale short compared with that for destruction by nuclear reactions, but similar calculations showed that for $T_9 \geq 5\cdot0$ it is not.

We therefore included proton inelastic and superelastic (inelastic with positive Q-value) scattering as a further means of communication between states. This had negligible effect for $T_9 < 4\cdot2$ but had a marked effect for $T_9 \geq 4\cdot8$, as is clear from Fig. 2. From these results we concluded that ^{52}Mn achieves a distribution within 10% of thermal at all temperatures. Emission and absorption

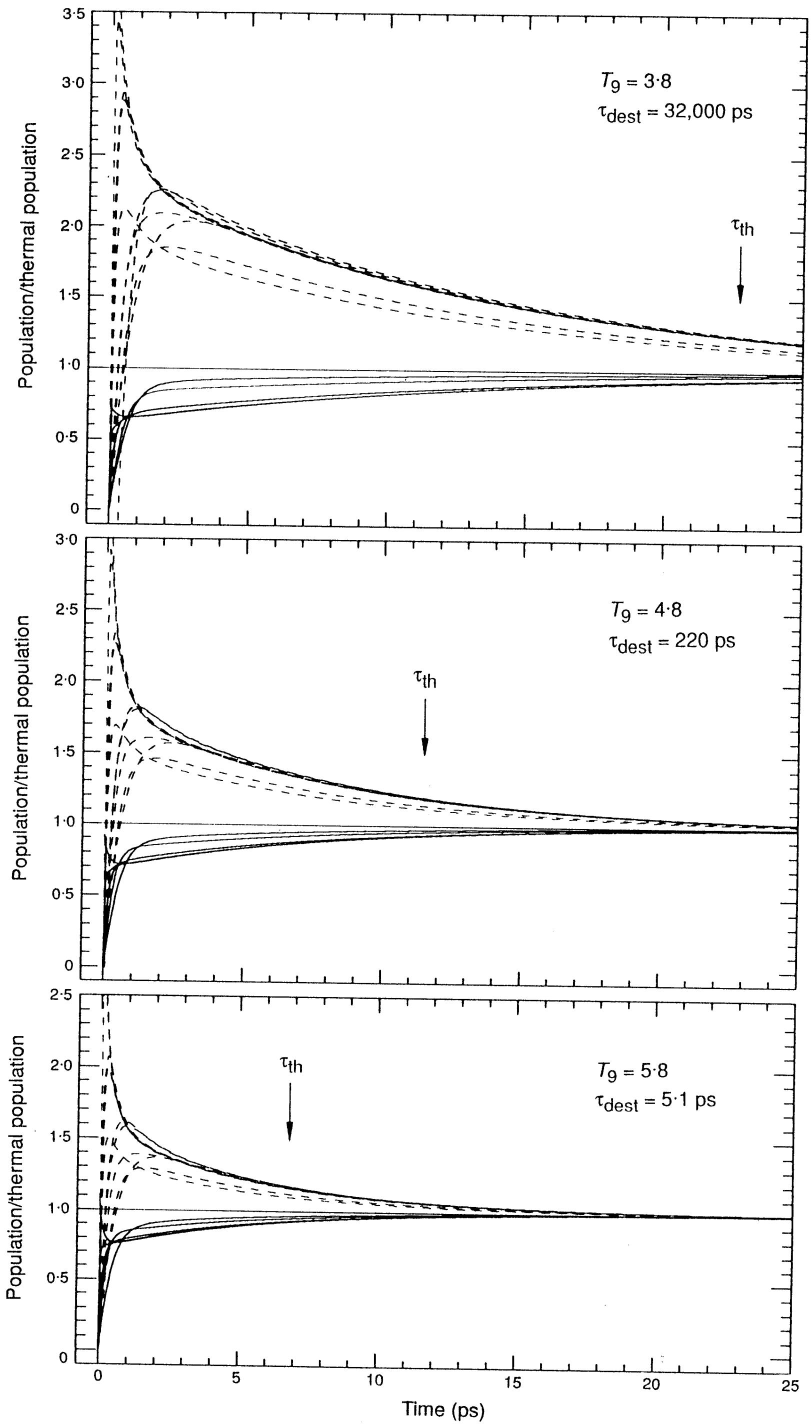

Fig. 1. The approach to thermalisation, by electromagnetic transitions only, of the ground state and first 19 excited states of ^{52}Mn, for the temperatures $T_9 = 3{\cdot}8, 4{\cdot}8$ and $5{\cdot}8$, as described in the text. The solid curves correspond to the high-spin states and the dashed curves to the low-spin states.

of electromagnetic radiation is the dominant mechanism for $T_9 < 4 \cdot 6$, and proton scattering the dominant mechanism for $T_9 > 5$. Other nuclear processes, coupled with their inverses [for example $^{52}Mn(p,n)^{52}Fe(n,p)^{52}Mn$], can serve only to speed up the approach to thermal equilibrium. We therefore conclude that ^{52}Mn can validly be treated as a single nucleus for the purposes of nucleosynthesis network calculations.

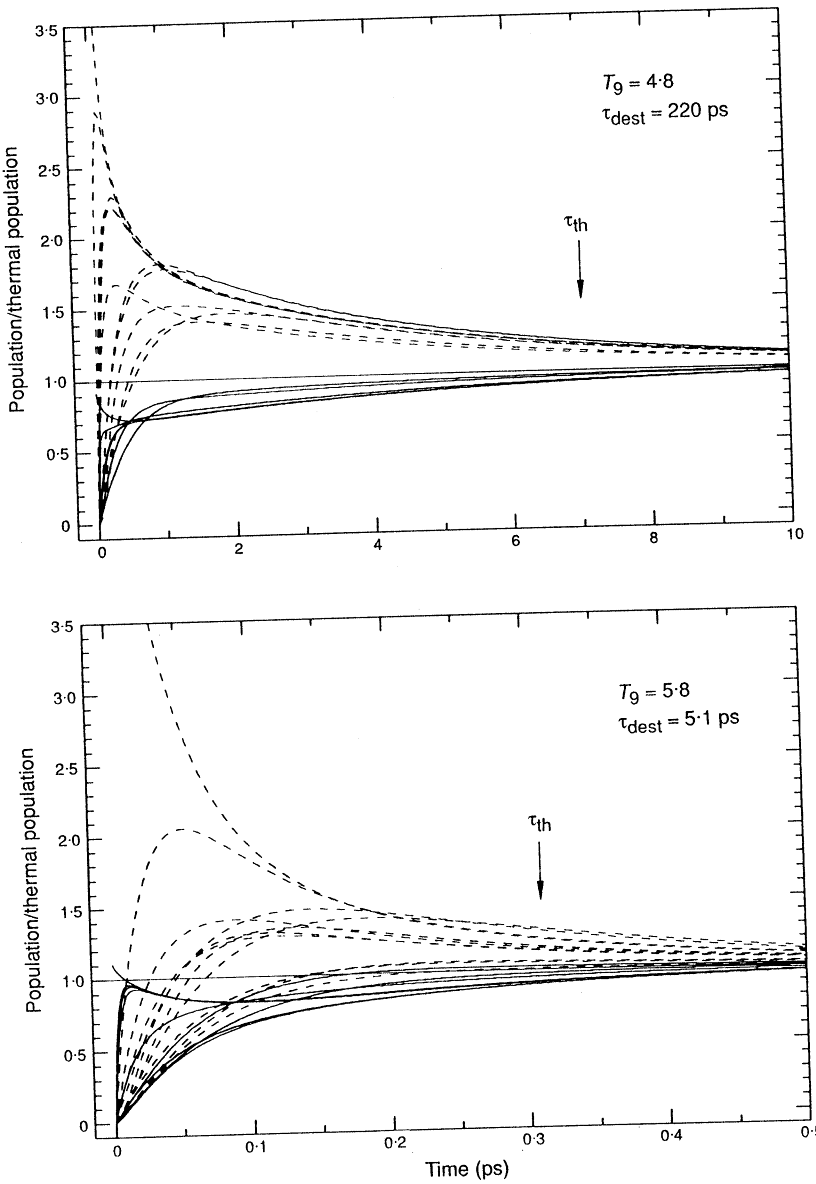

Fig. 2. The approach to thermalisation, by electromagnetic transitions and proton scattering, of the ground state and first 19 excited states of ^{52}Mn, for the temperatures $T_9 = 4 \cdot 8$ and $5 \cdot 8$, as described in the text. The solid curves correspond to the high-spin states and the dashed curves to the low-spin states.

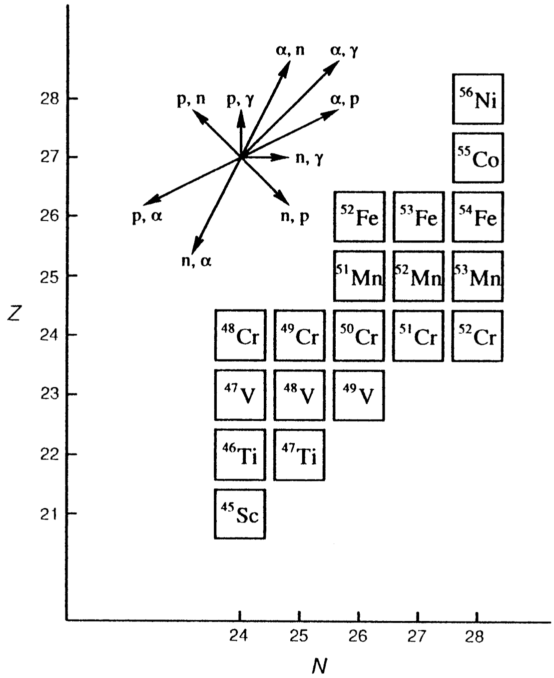

Fig. 3. Nuclei of importance in the later stages of explosive Si-burning, as described by Woosley *et al.* (1973), which have been treated as targets in rate calculations.

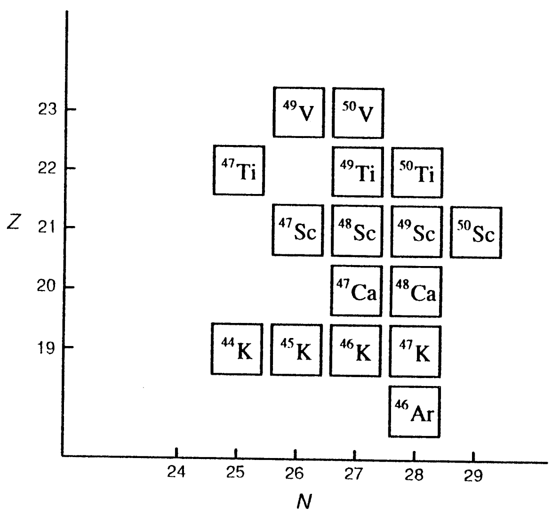

Fig. 4. Nuclei of importance in the explosive C-burning process of Howard *et al.* (1972), which have been treated as targets in rate calculations.

5. Stellar Reaction Rates

The nuclei, reactions on which are of greatest importance in the advance of nucleosynthesis to species with $N \sim 28$, are shown in Fig. 3 for silicon burning and in Fig. 4 for the process of Howard *et al.* (1972). We have calculated stellar reaction rates per mole, $N_{\rm A}\langle\sigma v\rangle^*$, for $(\rm n,\gamma)$, $(\rm n,p)$, $(\rm n,\alpha)$, $(\rm p,\gamma)$, $(\rm p,n)$, $(\rm p,\alpha)$, (α,γ), $(\alpha,\rm n)$, and $(\alpha,\rm p)$ reactions on each of these nuclei, for a range of temperatures from $T_9 = 0\cdot1$ to $T_9 = 10$. The results are given in Table 2.

For various reasons there are some gaps in Table 2. For some reactions at temperatures $T_9 \leq 1$, either the cross sections required were too small for HAUSER*4 to calculate or the rates too small for our rates program to calculate. For $^{52}\rm Fe(p,\gamma)^{53}Co$ the cross sections required were too small at all temperatures in the range. Cross sections of neutron-induced reactions on ^{46}Ar and ^{45,47}K were not accessible to calculation because HAUSER*4 requires at least ground-state spectroscopic information in every exit channel and this condition could not be satisfied. For proton-induced reactions on ^{56}Ni, our imaginary optical-model well specification becomes unphysical, making it impossible to calculate cross sections with HAUSER*4: a similar conclusion was reached by Tingwell *et al.* (1989).

We have compared the reaction rates in Table 2 with those in the compilation of Hoffman and Woosley (1992). For a vast majority of the reactions there is agreement to within a factor of 3 over the temperature range from $T_9 = 0\cdot5$ to $T_9 = 5$, the range of greatest significance for explosive nucleosynthesis and freeze-out. The factor of 3 corresponds to the limit of accuracy required for nucleosynthesis calculations (Woosley *et al.* 1978). In some cases the rates of Hoffman and Woosley are based on published experimental data, but the bulk are based on the statistical-model calculations of Woosley *et al.* (1975, 1978). Where there is significant disagreement between our rates and those of Hoffman and Woosley that are based on statistical-model cross sections, the disagreement may be attributed to (i) the different potential well specification used, particularly for $N = 28$ compound nuclei, (ii) the fact that we have much more nuclear spectroscopic data available for the particle channels than had Woosley *et al.* at the time their calculations were made, and (iii) the fact that the rates of reactions whose cross sections are very small compared with those of competing reactions with the same entrance channel are necessarily of doubtful reliability. Most cases for which disagreement by a factor > 3 occurs mainly at temperatures $T_9 < 1\cdot5$ fall in the third category.

Since our optical-model well parameters have been chosen specifically to fit experimental cross sections in the relevant mass range, generally to within a factor of $1\cdot5$, and since the greater the amount of spectroscopic data available and the less the dependence on a density-of-states formula the more reliable the cross section calculation, our rates should be an improvement on those of Woosley *et al.* However, where the rates are very small, we consider them to be too unreliable for any such claim to be made. Fortunately, such reactions are of very minor importance in the scheme of nucleosynthesis.

The greatest general disagreement between our rates and those of Hoffman and Woosley (1992) occurs with α-particle-induced reactions, most notably (α,γ) reactions. The approximately 20 reactions involved are fairly evenly divided between those with $N = 28$ and $N \neq 28$ compound nuclei. Most, if not all, of these reactions are of very minor significance for evolutionary nucleosynthesis because

Table 2. $N_A\langle\sigma v\rangle^*$ ($cm^3\,s^{-1}\,mol^{-1}$)

Target	T_9	n, γ	n, p	n, α	p, γ	p, n	p, α	α, γ	α, n	α, p
^{46}Ar	0.1				1.2E−16	1.5E−12				
	0.3				1.3E−08	1.8E−04				
	0.5				1.1E−05	1.4E−01		1.4E−20	6.7E−16	
	1.0				1.3E−02	1.8E+02	1.4E−14	6.8E−13	3.5E−08	1.2E−24
	1.5				3.5E−01	5.3E+03	2.2E−09	2.9E−09	1.6E−04	7.4E−16
	2.0				2.7E+00	4.3E+04	2.4E−06	5.0E−07	2.7E−02	3.1E−11
	2.5				1.2E+01	1.8E+05	2.7E−04	1.8E−05	9.8E−01	2.5E−08
	3.0				3.4E+01	5.5E+05	8.5E−03	2.5E−04	1.4E+01	2.6E−06
	4.0				1.6E+02	2.6E+06	9.3E−01	9.9E−03	5.3E+02	1.1E−03
	5.0				4.5E+02	7.6E+06	2.0E+01	1.2E−01	6.1E+03	5.6E−02
	7.0				1.8E+03	3.0E+07	9.5E+02	2.7E+00	1.3E+05	7.0E+00
	10.0				6.3E+03	9.5E+07	2.4E+04	3.9E+01	1.6E+06	4.3E+02
^{44}K	0.1	2.5E+06			1.8E−16	8.2E−13	2.0E−20			
	0.3	1.7E+06			2.8E−08	1.3E−04	1.7E−11	1.4E−27	3.0E−24	1.6E−26
	0.5	1.7E+06	2.7E−27		1.9E−05	9.3E−02	6.1E−08	3.1E−20	6.9E−17	4.5E−19
	1.0	1.7E+06	4.1E−12		3.1E−02	1.5E+02	1.1E−03	2.2E−12	5.4E−09	4.4E−11
	1.5	1.5E+06	1.5E−06	8.4E−13	1.0E+00	4.6E+03	1.7E−01	1.2E−08	3.0E−05	2.7E−07
	2.0	1.3E+06	1.4E−03	1.5E−08	8.4E+00	3.8E+04	4.3E+00	2.3E−06	6.2E−03	6.6E−05
	2.5	1.2E+06	1.1E−01	8.7E−06	3.6E+01	1.6E+05	4.2E+01	9.2E−05	2.6E−01	3.3E−03
	3.0	1.0E+06	2.2E+00	7.6E−04	1.1E+02	4.9E+05	2.3E+02	1.4E−03	4.2E+00	6.4E−02
	4.0	8.8E+05	1.1E+02	3.0E−01	4.9E+02	2.2E+06	2.5E+03	6.9E−02	2.1E+02	4.2E+00
	5.0	7.6E+05	1.4E+03	1.4E+01	1.4E+03	6.1E+06	1.3E+04	9.2E−01	2.9E+03	7.1E+01
	7.0	5.7E+05	2.6E+04	1.4E+03	4.9E+03	2.3E+07	1.0E+05	2.3E+01	7.5E+04	2.4E+03
	10.0	3.9E+05	2.5E+05	4.9E+04	1.5E+04	7.2E+07	6.3E+05	3.2E+02	1.1E+06	4.7E+04
^{45}K	0.1				1.5E−16	5.8E−13	3.8E−19			
	0.3				2.3E−08	9.6E−05	1.9E−10	9.3E−28	2.7E−24	1.6E−26
	0.5				2.1E−05	9.1E−02	4.0E−07	2.3E−20	7.3E−17	4.3E−19
	1.0				3.2E−02	1.4E+02	2.5E−03	1.6E−12	6.0E−09	3.1E−11
	1.5				9.6E−01	4.5E+03	2.1E−01	8.5E−09	3.6E−05	1.4E−07
	2.0				7.7E+00	3.7E+04	3.7E+00	1.7E−06	7.8E−03	2.6E−05
	2.5				3.2E+01	1.6E+05	2.9E+01	7.1E−05	3.3E−01	1.2E−03
	3.0				9.3E+01	4.8E+05	1.4E+02	1.1E−03	5.4E+00	2.3E−02
	4.0				4.1E+02	2.2E+06	1.3E+03	5.2E−02	2.6E+02	1.9E+00
	5.0				1.1E+03	6.2E+06	6.1E+03	6.7E−01	3.4E+03	3.7E+01
	7.0				4.2E+03	2.4E+07	4.7E+04	1.6E+01	8.2E+04	1.6E+03
	10.0				1.3E+04	7.5E+07	3.3E+05	2.3E+02	1.1E+06	3.5E+04
^{46}K	0.1	8.1E+05			6.5E−17	3.6E−13	7.9E−25			
	0.3	6.0E+05			1.6E−08	8.7E−05	6.3E−15	3.4E−28	3.2E−24	6.7E−28
	0.5	6.5E+05	3.4E−49		1.5E−05	8.7E−02	5.4E−11	8.1E−21	8.2E−17	2.9E−20
	1.0	7.3E+05	4.1E−23	3.2E−35	2.4E−02	1.4E+02	3.7E−06	5.7E−13	6.3E−09	4.2E−12
	1.5	7.5E+05	7.6E−14	1.8E−22	7.4E−01	4.4E+03	1.4E−03	3.3E−09	3.8E−05	2.9E−08
	2.0	7.4E+05	5.3E−09	1.1E−15	6.1E+00	3.7E+04	7.2E−02	7.0E−07	8.2E−03	6.0E−06
	2.5	7.0E+05	5.3E−06	2.1E−11	2.7E+01	1.6E+05	1.2E+00	2.9E−05	3.4E−01	2.3E−04
	3.0	6.6E+05	5.8E−04	2.0E−08	8.0E+01	4.8E+05	9.1E+00	4.6E−04	5.4E+00	3.7E−03
	4.0	5.9E+05	2.5E−01	1.4E−04	3.7E+02	2.2E+06	1.6E+02	2.2E−02	2.5E+02	2.2E−01
	5.0	5.4E+05	1.1E+01	3.5E−02	1.1E+03	6.4E+06	1.1E+03	2.9E−01	3.2E+03	4.3E+00
	7.0	4.4E+05	9.9E+02	2.1E+01	4.1E+03	2.5E+07	1.6E+04	7.4E+00	8.0E+04	2.6E+02
	10.0	2.8E+05	2.8E+04	2.0E+03	1.3E+04	8.0E+07	1.6E+05	1.1E+02	1.1E+06	9.2E+03

Table 2. (Continued)

Target	T_9	n, γ	n, p	n, α	p, γ	p, n	p, α	α, γ	α, n	α, p
^{47}K	0.1				5.7E−17	2.6E−13	4.2E−25			
	0.3				9.8E−09	5.1E−05	3.2E−15	1.3E−28	3.1E−24	3.2E−36
	0.5				9.1E−06	4.8E−02	2.7E−11	2.5E−21	7.0E−17	9.3E−25
	1.0				1.4E−02	7.8E+01	1.8E−06	2.2E−13	7.1E−09	6.8E−14
	1.5				4.5E−01	2.6E+03	6.3E−04	1.3E−09	4.3E−05	2.9E−09
	2.0				3.8E+00	2.3E+04	2.6E−02	2.5E−07	8.9E−03	1.4E−06
	2.5				1.7E+01	1.0E+05	3.5E−01	1.0E−05	3.6E−01	8.4E−05
	3.0				5.3E+01	3.3E+05	2.5E+00	1.5E−04	5.5E+00	1.6E−03
	4.0				2.7E+02	1.7E+06	3.8E+01	7.0E−03	2.5E+02	9.1E−02
	5.0				8.1E+02	5.1E+06	2.5E+02	9.1E−02	3.2E+03	1.3E+00
	7.0				3.5E+03	2.2E+07	3.8E+03	2.4E+00	8.0E+04	4.5E+01
	10.0				1.2E+04	7.5E+07	5.3E+04	4.2E+01	1.2E+06	1.6E+03
^{46}Ca	0.1	1.5E+05								
	0.3	1.6E+05			2.7E−05	1.0E−30				1.8E−40
	0.5	2.4E+05			3.3E−02	1.6E−15		2.0E−19	7.6E−18	1.1E−26
	1.0	3.7E+05	4.7E−32		4.7E+01	6.6E−04	5.3E−18	4.6E−12	1.3E−09	2.6E−14
	1.5	4.4E+05	2.5E−19	2.1E−21	9.9E+02	5.3E+00	2.8E−11	1.3E−08	1.0E−05	4.0E−09
	2.0	5.0E+05	1.0E−12	1.2E−14	5.6E+03	5.0E+02	1.5E−07	2.4E−06	2.7E−03	4.4E−06
	2.5	5.5E+05	1.3E−08	2.3E−10	1.7E+04	8.0E+03	4.7E−05	9.9E−05	1.3E−01	4.7E−04
	3.0	6.0E+05	8.4E−06	2.3E−07	3.7E+04	5.2E+04	3.1E−03	1.6E−03	2.3E+00	1.3E−02
	4.0	6.7E+05	3.5E−02	1.9E−03	9.6E+04	5.8E+05	9.6E−01	7.6E−02	1.2E+02	1.2E+00
	5.0	7.2E+05	5.8E+00	5.2E−01	1.5E+05	2.6E+06	4.2E+01	1.0E+00	1.8E+03	2.3E+01
	7.0	7.7E+05	2.0E+03	3.3E+02	2.0E+05	1.5E+07	4.2E+03	2.6E+01	5.0E+04	1.0E+03
	10.0	7.0E+05	1.3E+05	3.0E+04	1.4E+05	5.9E+07	1.5E+05	3.7E+02	7.7E+05	3.7E+04
^{47}Ca	0.1	6.7E+05			9.9E−17	7.9E−14				
	0.3	5.1E+05			2.1E−08	2.6E−05				1.0E−57
	0.5	5.5E+05	4.3E−59		2.4E−05	3.3E−02		2.5E−21	8.0E−18	3.7E−36
	1.0	6.2E+05	3.8E−28	3.2E−30	4.0E−02	6.6E+01	3.1E−19	2.0E−13	1.1E−09	1.8E−18
	1.5	6.5E+05	3.4E−17	1.7E−19	1.3E+00	2.4E+03	1.4E−12	1.6E−09	1.1E−05	9.0E−12
	2.0	6.7E+05	1.9E−11	1.2E−13	1.1E+01	2.2E+04	1.2E−08	3.9E−07	2.8E−03	4.2E−08
	2.5	6.9E+05	7.1E−08	6.7E−10	4.8E+01	1.0E+05	4.3E−06	1.8E−05	1.3E−01	9.4E−06
	3.0	7.1E+05	2.1E−05	3.1E−07	1.5E+02	3.1E+05	3.2E−04	2.9E−04	2.2E+00	4.2E−04
	4.0	7.5E+05	3.2E−02	1.1E−03	7.2E+02	1.6E+06	1.3E−01	1.5E−02	1.2E+02	6.5E−02
	5.0	8.1E+05	3.1E+00	1.9E−01	2.1E+03	4.7E+06	7.5E+00	2.1E−01	1.7E+03	1.7E+00
	7.0	9.1E+05	7.0E+02	9.1E+01	8.4E+03	1.9E+07	1.4E+03	5.7E+00	4.9E+04	1.3E+02
	10.0	8.3E+05	4.0E+04	8.2E+03	2.5E+04	6.5E+07	9.1E+04	9.0E+01	7.9E+05	8.8E+03
^{48}Ca	0.1	2.4E+04								
	0.3	2.6E+04			1.1E−05	1.4E−09				
	0.5	3.3E+04			1.2E−02	1.4E−04		4.2E−20	8.7E−18	7.9E−65
	1.0	4.2E+04	5.9E−54	1.6E−50	2.0E+01	5.5E+00		1.8E−12	1.5E−09	1.0E−31
	1.5	4.6E+04	6.4E−34	2.2E−32	3.8E+02	5.3E+02	1.1E−15	4.8E−09	1.2E−05	3.5E−20
	2.0	4.9E+04	1.1E−23	7.4E−23	1.8E+03	7.1E+03	4.7E−11	6.1E−07	2.9E−03	3.1E−14
	2.5	5.1E+04	2.1E−17	6.7E−17	4.7E+03	4.0E+04	5.5E−08	1.9E−05	1.3E−01	1.4E−10
	3.0	5.3E+04	3.7E−13	8.2E−13	8.7E+03	1.4E+05	1.0E−05	2.5E−04	2.2E+00	4.6E−08
	4.0	6.0E+04	9.5E−08	1.5E−07	1.9E+04	8.6E+05	1.4E−02	1.0E−02	1.2E+02	8.3E−05
	5.0	7.1E+04	2.1E−04	2.8E−04	2.9E+04	2.9E+06	1.6E+00	1.3E−01	1.7E+03	1.1E−02
	7.0	1.1E+05	1.8E+00	1.8E+00	4.3E+04	1.4E+07	6.4E+02	3.4E+00	5.0E+04	7.9E+00
	10.0	1.4E+05	1.1E+03	7.6E+02	3.6E+04	5.7E+07	5.4E+04	5.6E+01	8.4E+05	1.7E+03

Table 2. (Continued)

Target	T_9	n, γ	n, p	n, α	p, γ	p, n	p, α	α, γ	α, n	α, p
^{45}Sc	0.1	5.6E+06								
	0.3	3.6E+06			8.2E−06		2.9E−09		2.0E−38	
	0.5	3.4E+06	2.8E+03		1.3E−02	4.8E−21	1.6E−05	1.1E−19	3.9E−23	6.5E−19
	1.0	3.4E+06	2.4E+04	1.4E−10	2.5E+01	1.6E−06	1.6E−01	1.1E−11	3.1E−11	1.7E−10
	1.5	3.3E+06	1.2E+05	4.4E−06	5.8E+02	1.2E−01	9.3E+00	3.3E−08	1.0E−06	1.1E−06
	2.0	3.2E+06	4.0E+05	2.1E−03	3.3E+03	3.2E+01	1.0E+02	3.2E−06	4.2E−04	2.3E−04
	2.5	3.0E+06	9.6E+05	1.4E−01	9.6E+03	9.2E+02	5.4E+02	7.3E−05	2.6E−02	1.0E−02
	3.0	2.8E+06	1.9E+06	3.0E+00	2.0E+04	8.6E+03	1.8E+03	8.0E−04	5.4E−01	1.8E−01
	4.0	2.5E+06	4.9E+06	2.2E+02	5.0E+04	1.4E+05	1.0E+04	3.1E−02	3.8E+01	1.1E+01
	5.0	2.2E+06	9.4E+06	3.9E+03	8.3E+04	7.3E+05	3.4E+04	4.2E−01	6.5E+02	1.9E+02
	7.0	1.7E+06	2.2E+07	1.4E+05	1.4E+05	5.0E+06	2.1E+05	1.3E+01	2.3E+04	6.4E+03
	10.0	1.4E+06	5.3E+07	2.5E+06	1.9E+05	2.2E+07	1.5E+06	2.0E+02	4.3E+05	1.2E+05
^{47}Sc	0.1	3.5E+06								
	0.3	2.4E+06	3.9E−21		1.1E−06	8.0E−06	7.7E−13			
	0.5	2.4E+06	1.5E−12		3.6E−04	1.3E−02	2.7E−09	1.5E−20	8.4E−19	3.4E−20
	1.0	2.6E+06	1.3E−04	2.0E−22	2.8E−01	3.6E+01	6.8E−05	7.9E−13	2.7E−10	6.5E−12
	1.5	2.8E+06	2.7E−01	4.0E−14	8.5E+00	1.5E+03	1.3E−02	5.1E−09	2.9E−06	6.7E−08
	2.0	2.8E+06	2.1E+01	1.7E−09	6.5E+01	1.4E+04	3.8E−01	1.1E−06	9.2E−04	2.3E−05
	2.5	2.8E+06	3.5E+02	1.7E−06	2.5E+02	6.7E+04	4.7E+00	4.8E−05	4.9E−02	1.5E−03
	3.0	2.8E+06	2.6E+03	2.5E−04	6.4E+02	2.1E+05	3.3E+01	7.8E−04	9.3E−01	3.3E−02
	4.0	2.6E+06	3.7E+04	2.0E−01	2.3E+03	1.1E+06	5.6E+02	3.9E−02	5.6E+01	2.8E+00
	5.0	2.4E+06	2.0E+05	1.5E+01	5.3E+03	3.3E+06	4.0E+03	5.4E−01	8.8E+02	5.7E+01
	7.0	2.0E+06	1.5E+06	3.0E+03	1.5E+04	1.4E+07	5.3E+04	1.5E+01	2.9E+04	2.6E+03
	10.0	1.5E+06	8.3E+06	1.6E+05	3.6E+04	4.9E+07	5.2E+05	2.4E+02	5.1E+05	6.3E+04
^{48}Sc	0.1	2.1E+06	3.0E−06							
	0.3	1.6E+06	2.7E−02		8.1E−08	8.3E−06	1.7E−17			1.6E−32
	0.5	1.7E+06	1.2E+00	3.3E−38	7.0E−05	1.3E−02	6.3E−13	1.4E−21	9.1E−19	9.6E−24
	1.0	1.8E+06	1.2E+02	1.2E−19	9.3E−02	3.5E+01	3.0E−07	2.1E−13	2.8E−10	2.8E−14
	1.5	1.7E+06	1.4E+03	1.9E−12	2.7E+00	1.4E+03	2.5E−04	1.7E−09	3.0E−06	1.2E−09
	2.0	1.6E+06	6.4E+03	2.1E−08	2.1E+01	1.4E+04	1.9E−02	4.2E−07	9.2E−04	9.0E−07
	2.5	1.5E+06	1.8E+04	9.7E−06	8.4E+01	6.6E+04	4.1E−01	2.0E−05	4.9E−02	9.1E−05
	3.0	1.5E+06	4.0E+04	8.0E−04	2.4E+02	2.1E+05	4.2E+00	3.4E−04	9.2E−01	2.8E−03
	4.0	1.4E+06	1.3E+05	3.2E−01	1.0E+03	1.1E+06	1.2E+02	1.9E−02	5.6E+01	3.3E−01
	5.0	1.3E+06	2.8E+05	1.5E+01	2.8E+03	3.5E+06	1.1E+03	2.8E−01	9.0E+02	8.2E+00
	7.0	1.0E+06	7.4E+05	1.7E+03	9.6E+03	1.5E+07	2.0E+04	8.6E+00	3.0E+04	4.9E+02
	10.0	7.4E+05	2.4E+06	5.6E+04	2.5E+04	5.3E+07	2.3E+05	1.5E+02	5.6E+05	1.6E+04
^{49}Sc	0.1	3.5E+05								
	0.3	2.6E+05			1.5E−08	3.6E−06	1.6E−16			6.0E−50
	0.5	2.7E+05			1.7E−05	5.5E−03	1.7E−12	2.4E−21	1.0E−18	8.9E−33
	1.0	3.0E+05	3.6E−21		2.9E−02	1.5E+01	2.2E−07	1.4E−13	3.1E−10	4.5E−18
	1.5	3.1E+05	2.0E−12	7.6E−23	9.5E−01	6.0E+02	1.2E−04	6.5E−10	3.2E−06	3.3E−12
	2.0	3.1E+05	8.1E−08	5.0E−16	8.1E+00	6.1E+03	8.5E−03	1.5E−07	9.3E−04	8.2E−09
	2.5	3.2E+05	6.1E−05	1.1E−11	3.6E+01	3.1E+04	1.7E−01	6.5E−06	4.8E−02	1.6E−06
	3.0	3.3E+05	5.8E−03	1.3E−08	1.1E+02	1.1E+05	1.6E+00	1.1E−04	9.1E−01	7.3E−05
	4.0	3.6E+05	2.1E+00	1.3E−04	5.7E+02	6.2E+05	4.0E+01	6.3E−03	5.7E+01	1.3E−02
	5.0	4.0E+05	8.4E+01	4.7E−02	1.8E+03	2.1E+06	3.7E+02	9.7E−02	9.4E+02	4.1E−01
	7.0	4.9E+05	6.7E+03	4.9E+01	7.7E+03	1.1E+07	9.1E+03	3.2E+00	3.3E+04	3.6E+01
	10.0	4.9E+05	1.7E+05	7.7E+03	2.5E+04	4.3E+07	2.2E+05	5.7E+01	6.2E+05	2.6E+03

Table 2. (Continued)

Target	T_9	n, γ	n, p	n, α	p, γ	p, n	p, α	α, γ	α, n	α, p
^{50}Sc	0.1	4.1E+05								
	0.3	3.0E+05			1.2E−09	6.6E−06	1.5E−12			2.0E−58
	0.5	3.2E+05			1.7E−06	9.8E−03	6.6E−09	4.9E−22	1.1E−18	3.2E−37
	1.0	3.4E+05	2.9E−20		5.0E−03	3.1E+01	1.2E−04	9.5E−14	3.1E−10	1.3E−19
	1.5	3.3E+05	4.1E−12	1.2E−15	2.0E−01	1.3E+03	1.8E−02	7.8E−10	3.2E−06	6.1E−13
	2.0	3.2E+05	8.1E−08	8.7E−11	2.0E+00	1.4E+04	4.3E−01	2.0E−07	9.2E−04	3.0E−09
	2.5	3.0E+05	4.0E−05	1.2E−07	9.4E+00	6.8E+04	4.1E+00	9.4E−06	4.8E−02	7.8E−07
	3.0	2.9E+05	2.9E−03	2.1E−05	3.0E+01	2.2E+05	2.2E+01	1.7E−04	9.2E−01	4.1E−05
	4.0	2.8E+05	8.0E−01	1.9E−02	1.6E+02	1.2E+06	2.4E+02	1.0E−02	6.0E+01	8.9E−03
	5.0	2.6E+05	2.8E+01	1.5E+00	4.8E+02	3.9E+06	1.2E+03	1.6E−01	1.0E+03	3.2E−01
	7.0	2.3E+05	2.0E+03	2.6E+02	2.0E+03	1.7E+07	1.3E+04	5.2E+00	3.6E+04	3.6E+01
	10.0	1.5E+05	4.4E+04	1.1E+04	7.0E+03	6.2E+07	1.6E+05	9.2E+01	6.6E+05	2.3E+03
^{46}Ti	0.1	1.0E+06								
	0.3	8.8E+05			2.5E−06					5.9E−35
	0.5	1.2E+06			4.6E−03			8.3E−20	1.5E−40	1.3E−22
	1.0	1.9E+06	5.9E−06		7.1E+00		1.6E−24	3.0E−11	8.0E−18	1.5E−11
	1.5	2.3E+06	1.3E−01	1.2E−04	1.4E+02	6.7E−18	3.3E−15	1.4E−07	4.0E−10	4.8E−07
	2.0	2.5E+06	3.1E+01	3.6E−02	7.2E+02	2.5E−11	4.0E−10	1.7E−05	3.4E−06	2.1E−04
	2.5	2.7E+06	1.0E+03	1.7E+00	2.1E+03	2.6E−07	7.3E−07	4.0E−04	8.9E−04	1.3E−02
	3.0	2.8E+06	1.1E+04	3.0E+01	4.4E+03	1.5E−04	1.5E−04	4.1E−03	4.0E−02	2.7E−01
	4.0	2.8E+06	2.6E+05	1.6E+03	1.2E+04	4.7E−01	1.8E−01	1.1E−01	5.9E+00	1.8E+01
	5.0	2.9E+06	1.9E+06	2.3E+04	2.2E+04	6.7E+01	1.6E+01	1.2E+00	1.5E+02	3.1E+02
	7.0	2.8E+06	2.0E+07	6.5E+05	4.5E+04	2.0E+04	3.6E+03	2.9E+01	7.6E+03	1.0E+04
	10.0	2.4E+06	1.2E+08	8.3E+06	7.4E+04	1.3E+06	2.0E+05	3.9E+02	1.9E+05	1.8E+05
^{47}Ti	0.1	6.1E+06		2.8E+00						
	0.3	4.2E+06	1.1E−02	3.1E+00	2.6E−06					1.9E−32
	0.5	4.1E+06	1.1E+00	5.1E+00	5.2E−03			1.2E−20	7.9E−20	3.8E−22
	1.0	3.7E+06	3.3E+02	1.6E+01	1.3E+01	8.5E−11	2.0E−21	1.8E−12	4.5E−11	2.7E−12
	1.5	3.4E+06	5.7E+03	5.9E+01	3.4E+02	1.7E−04	1.4E−13	6.6E−09	6.2E−07	7.1E−08
	2.0	3.2E+06	3.5E+04	2.2E+02	2.1E+03	2.5E−01	3.7E−09	1.1E−06	2.2E−04	3.7E−05
	2.5	3.1E+06	1.3E+05	7.8E+02	6.7E+03	2.1E+01	3.0E−06	4.2E−05	1.4E−02	2.7E−03
	3.0	3.0E+06	3.4E+05	2.5E+03	1.5E+04	3.9E+02	3.8E−04	6.2E−04	2.9E−01	6.6E−02
	4.0	2.9E+06	1.4E+06	1.7E+04	4.4E+04	1.6E+04	2.7E−01	2.9E−02	2.1E+01	5.8E+00
	5.0	2.8E+06	3.8E+06	7.9E+04	8.6E+04	1.6E+05	2.0E+01	4.1E−01	3.6E+02	1.2E+02
	7.0	2.5E+06	1.5E+07	7.2E+05	1.8E+05	2.1E+06	3.5E+03	1.2E+01	1.3E+04	5.2E+03
	10.0	2.0E+06	5.3E+07	5.4E+06	2.8E+05	1.5E+07	1.9E+05	2.0E+02	2.6E+05	1.2E+05
^{48}Ti	0.1	5.3E+05								
	0.3	4.9E+05			2.2E−06	3.1E−72				5.5E−37
	0.5	7.0E+05	8.0E−34		4.0E−03	6.4E−40		1.0E−19	5.3E−26	4.4E−24
	1.0	1.1E+06	3.8E−14	1.9E−18	1.0E+01	1.4E−15	5.7E−22	5.3E−11	5.6E−12	1.6E−12
	1.5	1.3E+06	4.2E−07	4.8E−11	2.6E+02	2.1E−07	1.2E−13	3.3E−07	5.0E−07	4.0E−08
	2.0	1.4E+06	2.2E−03	6.5E−07	1.6E+03	2.8E−03	3.9E−09	3.8E−05	2.6E−04	1.7E−05
	2.5	1.5E+06	4.6E−01	3.3E−04	5.1E+03	9.0E−01	3.4E−06	7.7E−04	1.7E−02	1.2E−03
	3.0	1.6E+06	1.8E+01	2.7E−02	1.2E+04	4.2E+01	4.5E−04	6.3E−03	3.5E−01	3.1E−02
	4.0	1.6E+06	2.0E+03	9.9E+00	3.5E+04	5.3E+03	3.3E−01	1.3E−01	2.4E+01	3.0E+00
	5.0	1.7E+06	3.8E+04	4.1E+02	7.2E+04	9.6E+04	2.3E+01	1.2E+00	4.2E+02	6.4E+01
	7.0	1.6E+06	1.2E+06	3.3E+04	1.5E+05	2.4E+06	3.6E+03	2.9E+01	1.6E+04	3.2E+03
	10.0	1.4E+06	1.5E+07	7.8E+05	2.1E+05	2.3E+07	1.5E+05	4.7E+02	3.2E+05	8.9E+04

Table 2. (Continued)

Target	T_9	n, γ	n, p	n, α	p, γ	p, n	p, α	α, γ	α, n	α, p
^{49}Ti	0.1	1.9E+06				9.6E−64				
	0.3	1.5E+06	7.9E−27		2.6E−06	2.3E−17		4.9E−29		4.1E−49
	0.5	1.6E+06	2.5E−15		5.1E−03	5.2E−08		6.8E−21	1.0E−19	1.6E−31
	1.0	1.9E+06	9.9E−06	6.1E−09	1.4E+01	7.4E−01	1.7E−20	6.3E−13	6.0E−11	1.7E−16
	1.5	2.0E+06	4.7E−02	2.6E−05	3.8E+02	2.2E+02	6.4E−13	2.0E−09	8.6E−07	1.5E−10
	2.0	2.0E+06	5.0E+00	4.6E−03	2.2E+03	4.4E+03	1.2E−08	3.1E−07	3.1E−04	3.6E−07
	2.5	2.0E+06	1.0E+02	1.7E−01	6.4E+03	2.9E+04	7.9E−06	1.1E−05	1.8E−02	6.1E−05
	3.0	2.1E+06	9.1E+02	2.6E+00	1.3E+04	1.1E+05	8.4E−04	1.9E−04	3.7E−01	2.5E−03
	4.0	2.1E+06	1.7E+04	1.1E+02	2.9E+04	6.9E+05	4.7E−01	1.1E−02	2.7E+01	4.0E−01
	5.0	2.0E+06	1.1E+05	1.5E+03	4.4E+04	2.3E+06	2.8E+01	1.8E−01	4.8E+02	1.1E+01
	7.0	1.8E+06	9.6E+05	4.0E+04	6.5E+04	1.1E+07	3.8E+03	6.4E+00	1.9E+04	7.5E+02
	10.0	1.4E+06	5.8E+06	6.0E+05	8.4E+04	4.0E+07	1.6E+05	1.2E+02	4.0E+05	2.6E+04
^{50}Ti	0.1	1.4E+05							1.4E−93	
	0.3	1.4E+05			8.6E−07	8.4E−46			2.2E−33	
	0.5	1.9E+05			1.5E−03	4.0E−25		1.1E−19	5.2E−21	4.5E−52
	1.0	2.8E+05	2.8E−28	3.7E−25	4.5E+00	5.1E−09		7.9E−12	5.6E−11	1.5E−25
	1.5	3.2E+05	9.8E−17	1.3E−15	1.4E+02	2.1E−03	8.9E−14	1.9E−08	8.5E−07	5.2E−16
	2.0	3.5E+05	1.1E−10	2.2E−10	9.9E+02	1.5E+00	2.7E−09	2.3E−06	3.0E−04	6.0E−11
	2.5	3.8E+05	5.8E−07	5.1E−07	3.6E+03	8.5E+01	2.3E−06	6.0E−05	1.8E−02	9.0E−08
	3.0	4.1E+05	2.2E−04	1.2E−04	9.2E+03	1.3E+03	2.9E−04	6.7E−04	3.8E−01	1.4E−05
	4.0	4.6E+05	4.3E−01	1.6E−01	3.2E+04	4.0E+04	1.9E−01	2.0E−02	2.8E+01	1.1E−02
	5.0	5.0E+05	4.7E+01	1.5E+01	6.9E+04	3.4E+05	1.3E+01	2.2E−01	5.2E+02	6.7E−01
	7.0	5.5E+05	1.1E+04	3.0E+03	1.3E+05	4.2E+06	2.1E+03	6.1E+00	2.1E+04	9.9E+01
	10.0	4.9E+05	5.1E+05	1.2E+05	1.2E+05	2.7E+07	1.0E+05	1.1E+02	4.5E+05	5.7E+03
^{47}V	0.1	1.8E+06	1.8E+08	4.2E−05						
	0.3	2.0E+06	2.3E+08	6.5E−05	7.6E−07					
	0.5	2.3E+06	2.9E+08	1.1E−04	1.8E−03	2.6E−72		3.9E−23	4.3E−47	
	1.0	2.5E+06	3.7E+08	6.8E−03	3.4E+00	1.7E−32	2.1E−09	2.3E−14	2.0E−21	1.0E−11
	1.5	2.5E+06	4.1E+08	3.1E−01	6.5E+01	4.8E−19	4.8E−06	2.5E−10	1.0E−12	1.9E−07
	2.0	2.6E+06	4.4E+08	6.2E+00	3.2E+02	3.0E−12	6.4E−04	7.7E−08	3.1E−08	8.3E−05
	2.5	2.6E+06	4.6E+08	6.8E+01	8.5E+02	3.8E−08	2.2E−02	4.3E−06	1.8E−05	5.9E−03
	3.0	2.6E+06	4.9E+08	4.7E+02	1.7E+03	2.2E−05	3.2E−01	9.0E−05	1.4E−03	1.4E−01
	4.0	2.7E+06	5.3E+08	8.9E+03	4.1E+03	6.3E−02	1.6E+01	6.4E−03	4.3E−01	1.2E+01
	5.0	2.8E+06	5.8E+08	7.3E+04	7.1E+03	7.7E+00	2.5E+02	1.1E−01	1.6E+01	2.4E+02
	7.0	2.9E+06	6.7E+08	1.2E+06	1.4E+04	2.0E+03	9.7E+03	4.3E+00	1.3E+03	1.0E+04
	10.0	2.9E+06	8.0E+08	1.1E+07	2.3E+04	1.2E+05	2.3E+05	8.3E+01	4.5E+04	2.2E+05
^{48}V	0.1	3.3E+06	1.4E+08	3.3E+00						
	0.3	3.2E+06	1.6E+08	4.4E+00	8.2E−07				1.9E−36	
	0.5	3.7E+06	2.0E+08	6.9E+00	2.1E−03	2.1E−18	6.4E−26		2.9E−23	9.6E−21
	1.0	4.2E+06	2.5E+08	2.6E+01	6.5E+00	5.9E−06	1.9E−13	1.3E−13	2.1E−12	8.9E−12
	1.5	4.2E+06	2.8E+08	1.4E+02	1.8E+02	9.9E−02	2.7E−08	1.1E−09	5.9E−08	1.5E−07
	2.0	3.9E+06	2.9E+08	6.9E+02	1.1E+03	1.3E+01	2.7E−05	3.3E−07	2.8E−05	6.6E−05
	2.5	3.6E+06	3.0E+08	2.8E+03	3.2E+03	2.7E+02	2.9E−03	1.8E−05	2.1E−03	4.5E−03
	3.0	3.3E+06	3.1E+08	9.1E+03	6.6E+03	2.0E+03	9.0E−02	3.5E−04	5.2E−02	1.0E−01
	4.0	2.8E+06	3.2E+08	6.2E+04	1.6E+04	2.8E+04	1.0E+01	2.3E−02	4.8E+00	8.3E+00
	5.0	2.5E+06	3.3E+08	2.6E+05	2.7E+04	1.4E+05	2.3E+02	3.8E−01	9.9E+01	1.6E+02
	7.0	2.0E+06	3.5E+08	1.8E+06	4.7E+04	9.4E+05	1.1E+04	1.3E+01	4.6E+03	6.9E+03
	10.0	1.5E+06	3.8E+08	9.2E+06	6.5E+04	4.4E+06	2.1E+05	2.5E+02	1.1E+05	1.6E+05

Table 2. (Continued)

Target	T_9	n, γ	n, p	n, α	p, γ	p, n	p, α	α, γ	α, n	α, p
^{49}V	0.1	8.1E+06	4.9E+06							
	0.3	5.4E+06	3.7E+06		8.5E-07		6.4E-18			
	0.5	5.0E+06	4.0E+06		2.1E-03	4.2E-26	1.4E-12		1.1E-28	
	1.0	4.6E+06	5.1E+06	3.5E-12	6.7E+00	1.7E-09	8.3E-07	1.7E-12	1.4E-13	1.2E-11
	1.5	4.3E+06	6.4E+06	2.6E-07	1.9E+02	9.5E-04	4.3E-04	1.2E-08	3.5E-08	2.0E-07
	2.0	4.0E+06	8.1E+06	2.3E-04	1.2E+03	7.5E-01	2.4E-02	2.2E-06	3.3E-05	7.0E-05
	2.5	3.9E+06	1.0E+07	2.4E-02	4.1E+03	4.2E+01	4.3E-01	7.5E-05	3.0E-03	3.9E-03
	3.0	3.7E+06	1.2E+07	7.4E-01	9.2E+03	6.3E+02	4.1E+00	1.0E-03	7.8E-02	8.1E-02
	4.0	3.4E+06	1.8E+07	8.6E+01	2.6E+04	1.9E+04	1.1E+02	4.2E-02	7.0E+00	6.3E+00
	5.0	3.2E+06	2.5E+07	2.0E+03	5.0E+04	1.5E+05	1.1E+03	5.4E-01	1.4E+02	1.3E+02
	7.0	2.9E+06	4.7E+07	9.4E+04	1.0E+05	1.7E+06	2.1E+04	1.5E+01	6.9E+03	5.7E+03
	10.0	2.5E+06	1.1E+08	1.9E+06	1.7E+05	1.2E+07	3.0E+05	2.6E+02	1.7E+05	1.3E+05
^{50}V	0.1	3.6E+06	8.6E+02							
	0.3	3.1E+06	1.4E+04		6.8E-07	1.1E-09	1.9E-22			
	0.5	3.5E+06	4.3E+04	3.3E-11	1.6E-03	2.8E-05	5.3E-16	3.3E-21	8.4E-21	2.5E-23
	1.0	3.8E+06	4.1E+05	3.4E-06	6.0E+00	9.7E-01	5.2E-09	1.3E-12	1.2E-11	1.6E-13
	1.5	3.5E+06	1.4E+06	2.0E-03	1.8E+02	1.1E+02	1.5E-05	7.2E-09	2.3E-07	7.5E-09
	2.0	3.2E+06	2.8E+06	1.3E-01	1.1E+03	1.9E+03	2.5E-03	9.5E-07	9.6E-05	5.1E-06
	2.5	3.0E+06	4.1E+06	2.4E+00	3.6E+03	1.3E+04	8.4E-02	2.9E-05	6.3E-03	4.7E-04
	3.0	2.7E+06	5.5E+06	2.3E+01	7.8E+03	5.0E+04	1.2E+00	4.1E-04	1.4E-01	1.4E-02
	4.0	2.4E+06	8.3E+06	5.8E+02	2.1E+04	3.4E+05	4.8E+01	2.1E-02	1.2E+01	1.6E+00
	5.0	2.1E+06	1.1E+07	5.4E+03	3.7E+04	1.2E+06	6.1E+02	3.4E-01	2.3E+02	3.9E+01
	7.0	1.7E+06	1.9E+07	9.7E+04	6.8E+04	6.5E+06	1.6E+04	1.2E+01	1.1E+04	2.2E+03
	10.0	1.2E+06	3.7E+07	1.0E+06	9.4E+04	2.6E+07	2.4E+05	2.4E+02	2.4E+05	6.5E+04
^{51}V	0.1	1.9E+06				1.1E-71				
	0.3	1.3E+06			3.0E-07	2.6E-20	7.7E-18		1.3E-39	
	0.5	1.4E+06	2.1E-20		7.1E-04	6.7E-10	9.1E-13	1.2E-20	5.0E-24	1.2E-22
	1.0	1.4E+06	2.5E-08	2.0E-19	2.6E+00	5.7E-02	4.5E-07	6.8E-12	6.4E-12	4.1E-13
	1.5	1.4E+06	7.5E-04	4.6E-12	8.9E+01	2.9E+01	1.3E-04	1.9E-08	2.2E-07	2.8E-09
	2.0	1.4E+06	2.0E-01	6.7E-08	6.0E+02	7.3E+02	5.5E-03	1.4E-06	9.9E-05	1.1E-06
	2.5	1.4E+06	7.2E+00	3.7E-05	1.9E+03	5.6E+03	1.0E-01	2.5E-05	6.7E-03	8.5E-05
	3.0	1.3E+06	8.9E+01	3.3E-03	4.1E+03	2.4E+04	1.1E+00	2.3E-04	1.6E-01	2.3E-03
	4.0	1.3E+06	2.6E+03	1.5E+00	1.0E+04	1.7E+05	3.8E+01	7.9E-03	1.4E+01	2.6E-01
	5.0	1.3E+06	2.3E+04	8.1E+01	1.8E+04	6.8E+05	4.6E+02	1.2E-01	2.9E+02	6.6E+00
	7.0	1.2E+06	4.1E+05	1.1E+04	3.4E+04	4.0E+06	1.4E+04	4.4E+00	1.4E+04	4.2E+02
	10.0	1.1E+06	4.6E+06	4.4E+05	5.8E+04	1.8E+07	3.0E+05	8.9E+01	3.2E+05	1.6E+04
^{48}Cr	0.1	1.2E+06	6.1E+07							
	0.3	9.6E+05	6.1E+07							
	0.5	1.0E+06	7.6E+07						5.7E-77	2.6E-22
	1.0	1.3E+06	1.2E+08		3.6E-01	4.3E-62	2.0E-40	1.1E-12	4.0E-35	1.2E-12
	1.5	1.5E+06	1.6E+08	7.0E+00	5.9E+00	1.8E-38	4.8E-26	1.5E-08	3.9E-21	4.2E-08
	2.0	1.6E+06	2.2E+08	8.7E+01	2.8E+01	1.4E-26	2.3E-18	4.2E-06	4.0E-14	2.6E-05
	2.5	1.6E+06	2.8E+08	5.8E+02	7.7E+01	2.1E-19	1.6E-13	1.8E-04	6.4E-10	2.3E-03
	3.0	1.6E+06	3.5E+08	2.6E+03	1.6E+02	1.3E-14	3.8E-10	2.7E-03	4.0E-07	6.1E-02
	4.0	1.6E+06	4.9E+08	2.5E+04	4.0E+02	1.3E-08	9.9E-06	1.2E-01	1.2E-03	6.2E+00
	5.0	1.5E+06	6.4E+08	1.3E+05	7.3E+02	5.3E-05	5.8E-03	1.6E+00	1.5E-01	1.4E+02
	7.0	1.4E+06	9.1E+08	1.4E+06	1.7E+03	6.5E-01	1.0E+01	4.2E+01	4.0E+01	6.9E+03
	10.0	1.3E+06	1.3E+09	1.0E+07	3.8E+03	5.9E+02	2.8E+03	5.3E+02	2.9E+03	1.8E+05

Table 2. (Continued)

Target	T_9	n, γ	n, p	n, α	p, γ	p, n	p, α	α, γ	α, n	α, p
^{49}Cr	0.1	9.0E+05	1.7E+08	2.7E+04						
	0.3	1.2E+06	2.5E+08	4.2E+04	2.0E−07				4.5E−46	
	0.5	1.5E+06	3.5E+08	6.4E+04	5.9E−04	3.5E−75	2.5E−55		4.8E−28	1.0E−21
	1.0	1.9E+06	4.5E+08	1.1E+05	1.8E+00	6.5E−34	4.7E−29	6.2E−14	4.9E−14	2.5E−12
	1.5	2.0E+06	5.0E+08	1.7E+05	4.3E+01	5.7E−20	4.6E−19	3.2E−10	7.1E−09	5.7E−08
	2.0	2.1E+06	5.4E+08	2.4E+05	2.3E+02	6.3E−13	1.4E−13	6.4E−08	5.8E−06	2.8E−05
	2.5	2.2E+06	5.7E+08	3.5E+05	6.9E+02	1.1E−08	5.4E−10	2.8E−06	4.8E−04	2.1E−03
	3.0	2.2E+06	6.0E+08	5.0E+05	1.5E+03	8.0E−06	2.2E−07	5.1E−05	1.2E−02	5.5E−02
	4.0	2.3E+06	6.6E+08	1.0E+06	4.0E+03	3.1E−02	8.8E−04	3.3E−03	9.0E−01	5.4E+00
	5.0	2.4E+06	7.2E+08	2.1E+06	7.5E+03	4.5E+00	2.0E−01	5.7E−02	1.6E+01	1.2E+02
	7.0	2.5E+06	8.1E+08	6.8E+06	1.6E+04	1.4E+03	1.6E+02	2.2E+00	6.7E+02	6.6E+03
	10.0	2.4E+06	9.0E+08	2.2E+07	2.8E+04	8.9E+04	2.5E+04	4.6E+01	1.7E+04	1.8E+05
^{50}Cr	0.1	1.6E+06								
	0.3	1.3E+06			2.7E−07					
	0.5	1.8E+06			7.8E−04	9.3E−75		1.5E−21	1.3E−45	4.3E−23
	1.0	2.8E+06	7.7E−01		2.1E+00	1.6E−33	1.3E−27	1.9E−12	3.6E−20	1.1E−12
	1.5	3.3E+06	2.6E+02	1.9E−04	5.0E+01	2.1E−19	2.7E−17	2.3E−08	1.2E−11	4.8E−08
	2.0	3.5E+06	7.9E+03	4.3E−02	3.0E+02	3.0E−12	1.0E−11	5.5E−06	2.5E−07	2.9E−05
	2.5	3.6E+06	7.5E+04	1.8E+00	9.3E+02	6.3E−08	4.0E−08	2.1E−04	1.1E−04	2.3E−03
	3.0	3.7E+06	3.7E+05	2.9E+01	2.1E+03	4.8E−05	1.3E−05	2.9E−03	6.5E−03	5.5E−02
	4.0	3.7E+06	3.1E+06	1.4E+03	6.1E+03	2.0E−01	2.7E−02	1.1E−01	1.3E+00	4.8E+00
	5.0	3.6E+06	1.2E+07	1.8E+04	1.2E+04	3.2E+01	3.5E+00	1.2E+00	3.8E+01	1.0E+02
	7.0	3.4E+06	6.9E+07	4.4E+05	2.8E+04	1.1E+04	1.1E+03	3.1E+01	2.2E+03	5.3E+03
	10.0	2.7E+06	2.6E+08	5.1E+06	5.1E+04	7.7E+05	8.3E+04	4.6E+02	5.8E+04	1.5E+05
^{51}Cr	0.1	3.6E+06	1.6E+06	1.4E+01						
	0.3	3.3E+06	1.7E+06	2.0E+01	2.5E−07					2.1E−35
	0.5	3.9E+06	2.2E+06	3.4E+01	8.3E−04	1.1E−32		1.1E−21	3.7E−22	6.6E−24
	1.0	4.7E+06	3.2E+06	9.1E+01	3.5E+00	2.3E−12	6.6E−22	1.0E−12	1.5E−12	4.7E−13
	1.5	4.9E+06	4.3E+06	2.4E+02	1.2E+02	1.5E−05	5.8E−14	7.7E−09	4.3E−08	1.9E−08
	2.0	5.0E+06	5.9E+06	7.1E+02	8.5E+02	4.3E−02	1.8E−09	1.4E−06	2.3E−05	1.0E−05
	2.5	5.0E+06	7.9E+06	2.0E+03	3.0E+03	5.1E+00	1.6E−06	4.6E−05	1.8E−03	7.4E−04
	3.0	5.0E+06	1.0E+07	5.5E+03	7.5E+03	1.3E+02	2.2E−04	5.5E−04	4.7E−02	1.9E−02
	4.0	4.7E+06	1.7E+07	3.0E+04	2.4E+04	6.9E+03	1.7E−01	1.8E−02	4.7E+00	2.0E+00
	5.0	4.3E+06	2.6E+07	1.1E+05	4.9E+04	7.7E+04	1.3E+01	2.0E−01	1.0E+02	5.1E+01
	7.0	3.5E+06	4.7E+07	8.3E+05	1.1E+05	1.2E+06	2.5E+03	6.1E+00	5.3E+03	3.2E+03
	10.0	2.5E+06	8.8E+07	5.1E+06	1.7E+05	9.0E+06	1.4E+05	1.2E+02	1.3E+05	9.6E+04
^{52}Cr	0.1	7.1E+05								
	0.3	6.2E+05			8.4E−08	1.4E−83			2.8E−57	1.6E−55
	0.5	8.4E+05			2.5E−04	1.5E−47		1.5E−21	3.7E−33	5.5E−34
	1.0	1.2E+06	1.5E−14	9.8E−16	9.3E−01	1.4E−19	2.6E−23	3.0E−12	6.4E−15	1.0E−16
	1.5	1.4E+06	2.0E−07	2.0E−09	3.1E+01	3.3E−10	1.6E−14	6.0E−08	1.0E−08	1.6E−10
	2.0	1.6E+06	1.2E−03	8.0E−06	2.3E+02	1.9E−05	9.6E−10	1.7E−05	1.8E−05	3.7E−07
	2.5	1.7E+06	2.9E−01	1.9E−03	8.8E+02	1.4E−02	1.2E−06	5.9E−04	2.1E−03	5.5E−05
	3.0	1.8E+06	1.3E+01	1.0E−01	2.3E+03	1.3E+00	1.9E−04	6.8E−03	6.2E−02	2.1E−03
	4.0	2.0E+06	1.8E+03	2.2E+01	8.8E+03	3.7E+02	2.0E−01	1.6E−01	6.9E+00	3.7E−01
	5.0	2.1E+06	3.9E+04	7.7E+02	2.1E+04	1.1E+04	1.7E+01	1.1E+00	1.6E+02	1.3E+01
	7.0	1.9E+06	1.3E+06	5.3E+04	5.9E+04	4.9E+05	3.4E+03	1.3E+01	7.9E+03	1.2E+03
	10.0	1.5E+06	1.6E+07	1.1E+06	9.6E+04	6.2E+06	1.5E+05	1.8E+02	1.9E+05	4.3E+04

Table 2. (Continued)

Target	T_9	n, γ	n, p	n, α	p, γ	p, n	p, α	α, γ	α, n	α, p
^{51}Mn	0.1	9.4E+05	1.3E+08	1.4E−04						
	0.3	1.3E+06	2.0E+08	4.4E−04	8.1E−08			2.9E−33	2.9E−95	
	0.5	1.7E+06	2.8E+08	1.4E−03	3.2E−04			1.1E−23	1.5E−55	1.7E−22
	1.0	2.1E+06	3.8E+08	3.3E−02	1.0E+00	1.6E−35	1.6E−15	1.6E−14	2.5E−25	6.5E−13
	1.5	2.3E+06	4.4E+08	6.4E−01	2.6E+01	4.7E−21	3.8E−10	2.5E−10	3.5E−15	2.0E−08
	2.0	2.4E+06	4.9E+08	8.6E+00	1.4E+02	9.7E−14	5.8E−07	9.5E−08	4.3E−10	1.2E−05
	2.5	2.5E+06	5.3E+08	8.0E+01	4.2E+02	2.6E−09	8.8E−05	5.6E−06	5.2E−07	1.0E−03
	3.0	2.6E+06	5.7E+08	5.2E+02	8.9E+02	2.3E−06	3.7E−03	1.1E−04	6.5E−05	2.9E−02
	4.0	2.7E+06	6.5E+08	9.3E+03	2.3E+03	1.2E−02	6.9E−01	7.9E−03	3.6E−02	3.4E+00
	5.0	2.7E+06	7.3E+08	7.5E+04	4.3E+03	2.2E+00	2.3E+01	1.4E−01	2.1E+00	8.6E+01
	7.0	2.8E+06	8.7E+08	1.2E+06	8.5E+03	8.2E+02	1.9E+03	5.9E+00	3.0E+02	5.1E+03
	10.0	2.6E+06	1.0E+09	1.2E+07	1.4E+04	6.3E+04	7.0E+04	1.3E+02	1.6E+04	1.4E+05
^{52}Mn	0.1	1.5E+06	1.2E+07	1.9E+01						
	0.3	1.9E+06	1.9E+07	3.4E+01	8.2E−08	2.6E−47			6.5E−43	
	0.5	2.8E+06	2.9E+07	6.4E+01	3.3E−04	8.0E−26		1.1E−22	1.1E−26	6.8E−23
	1.0	3.9E+06	5.1E+07	2.1E+02	1.5E+00	1.4E−09	9.6E−15	1.9E−13	5.8E−14	4.2E−13
	1.5	4.3E+06	7.1E+07	7.0E+02	4.9E+01	3.9E−04	2.1E−09	2.2E−09	3.7E−09	1.5E−08
	2.0	4.4E+06	9.2E+07	2.4E+03	3.4E+02	2.3E−01	3.0E−06	5.3E−07	2.1E−06	9.4E−06
	2.5	4.3E+06	1.1E+08	7.4E+03	1.1E+03	1.1E+01	4.2E−04	2.3E−05	1.7E−04	8.5E−04
	3.0	4.1E+06	1.3E+08	2.0E+04	2.6E+03	1.5E+02	1.5E−02	3.7E−04	5.0E−03	2.4E−02
	4.0	3.7E+06	1.7E+08	9.8E+04	7.5E+03	4.1E+03	2.3E+00	1.9E−02	7.9E−01	2.7E+00
	5.0	3.2E+06	1.9E+08	3.4E+05	1.4E+04	3.1E+04	6.2E+01	2.9E−01	2.5E+01	6.4E+01
	7.0	2.5E+06	2.4E+08	2.0E+06	2.6E+04	3.2E+05	3.9E+03	1.0E+01	1.8E+03	3.7E+03
	10.0	1.7E+06	2.8E+08	8.6E+06	3.8E+04	1.9E+06	1.1E+05	2.0E+02	5.7E+04	1.0E+05
^{53}Mn	0.1	6.9E+06	1.4E+05							
	0.3	4.7E+06	1.8E+05		2.6E−08					
	0.5	4.8E+06	3.4E+05		9.2E−05	3.1E−38	3.5E−19	1.2E−22	5.2E−40	6.9E−23
	1.0	5.2E+06	8.5E+05	4.8E−10	4.7E−01	2.7E−15	7.2E−11	2.3E−13	5.6E−18	4.5E−13
	1.5	5.3E+06	1.5E+06	6.2E−06	2.0E+01	1.4E−07	6.0E−07	3.7E−09	1.6E−10	1.7E−08
	2.0	5.2E+06	2.3E+06	2.1E−03	1.7E+02	9.6E−04	1.6E−04	1.2E−06	1.1E−06	1.0E−05
	2.5	5.1E+06	3.5E+06	1.3E−01	6.9E+02	1.9E−01	7.7E−03	5.6E−05	2.5E−04	8.0E−04
	3.0	5.0E+06	5.0E+06	2.8E+00	1.9E+03	6.7E+00	1.4E−01	8.8E−04	1.1E−02	2.0E−02
	4.0	4.8E+06	9.7E+06	2.2E+02	7.1E+03	5.7E+02	9.1E+00	3.5E−02	1.9E+00	2.0E+00
	5.0	4.6E+06	1.7E+07	4.4E+03	1.7E+04	8.3E+03	1.7E+02	3.9E−01	5.3E+01	4.5E+01
	7.0	4.2E+06	4.7E+07	1.9E+05	4.6E+04	1.9E+05	8.4E+03	8.6E+00	3.5E+03	2.4E+03
	10.0	3.5E+06	1.4E+08	3.7E+06	9.1E+04	1.9E+06	2.4E+05	1.1E+02	1.1E+05	6.1E+04
^{52}Fe	0.1	8.6E+05	4.3E+07	6.1E−01						
	0.3	7.3E+05	5.2E+07	5.5E−01						
	0.5	8.1E+05	7.5E+07	1.2E+00				2.7E−23	7.2E−82	5.1E−25
	1.0	9.9E+05	1.3E+08	1.2E+01		1.8E−64	4.7E−41	1.4E−13	1.2E−37	1.1E−14
	1.5	1.2E+06	1.9E+08	9.0E+01		4.7E−40	1.2E−26	5.2E−09	6.1E−23	9.3E−10
	2.0	1.3E+06	2.4E+08	5.6E+02		8.9E−28	6.5E−19	3.2E−06	1.2E−15	1.1E−06
	2.5	1.3E+06	3.0E+08	2.4E+03		2.2E−20	5.0E−14	2.6E−04	2.7E−11	1.5E−04
	3.0	1.4E+06	3.6E+08	8.1E+03		1.9E−15	1.2E−10	6.5E−03	2.0E−08	6.2E−03
	4.0	1.4E+06	4.9E+08	5.2E+04		2.9E−09	3.5E−06	5.3E−01	6.6E−05	1.1E+00
	5.0	1.3E+06	6.1E+08	2.0E+05		1.5E−05	2.3E−03	9.2E+00	7.8E−03	3.4E+01
	7.0	1.2E+06	8.7E+08	1.5E+06		2.5E−01	5.0E+00	2.9E+02	1.8E+00	2.7E+03
	10.0	1.0E+06	1.3E+09	9.7E+06		3.0E+02	1.8E+03	3.8E+03	1.5E+02	9.6E+04

Table 2. (Continued)

Target	T_9	n, γ	n, p	n, α	p, γ	p, n	p, α	α, γ	α, n	α, p
^{53}Fe	0.1	1.1E+05	1.5E+07	5.5E+03						
	0.3	4.1E+05	4.6E+07	2.6E+04	2.8E−08		7.5E−90			
	0.5	8.6E+05	9.0E+07	6.3E+04	1.3E−04	2.6E−81	1.1E−57		1.1E−29	
	1.0	1.7E+06	1.7E+08	1.6E+05	4.9E−01	5.5E−37	2.2E−30	5.8E−15	1.9E−15	1.5E−13
	1.5	2.1E+06	2.2E+08	2.5E+05	1.3E+01	5.2E−22	8.1E−20	7.0E−11	2.7E−10	5.9E−09
	2.0	2.4E+06	2.6E+08	3.7E+05	8.2E+01	1.9E−14	5.2E−14	2.1E−08	2.1E−07	4.1E−06
	2.5	2.5E+06	2.8E+08	5.3E+05	2.6E+02	7.1E−10	3.0E−10	1.0E−06	1.8E−05	4.1E−04
	3.0	2.6E+06	3.0E+08	7.5E+05	6.0E+02	8.1E−07	1.5E−07	1.9E−05	5.3E−04	1.3E−02
	4.0	2.5E+06	3.3E+08	1.4E+06	1.8E+03	5.7E−03	6.1E−04	1.2E−03	7.3E−02	1.8E+00
	5.0	2.4E+06	3.5E+08	2.6E+06	3.5E+03	1.2E+00	1.4E−01	2.3E−02	2.2E+00	5.0E+01
	7.0	2.2E+06	3.8E+08	6.9E+06	8.3E+03	5.2E+02	1.1E+02	9.6E−01	2.0E+02	3.4E+03
	10.0	1.7E+06	4.1E+08	2.0E+07	1.7E+04	4.5E+04	2.0E+04	2.1E+01	8.9E+03	1.1E+05
^{54}Fe	0.1	1.8E+06								
	0.3	1.5E+06			7.5E−09					1.1E−46
	0.5	2.0E+06			3.0E−05			2.6E−23	4.7E−53	9.5E−30
	1.0	2.9E+06	3.9E+01		1.3E−01	5.7E−37		1.6E−13	1.5E−23	3.4E−15
	1.5	3.4E+06	2.5E+03	7.3E−04	4.4E+00	1.0E−21	1.3E−17	4.9E−09	1.1E−13	1.5E−09
	2.0	3.7E+06	3.5E+04	8.8E−02	3.2E+01	5.0E−14	4.1E−12	2.1E−06	1.0E−08	2.4E−06
	2.5	3.9E+06	2.2E+05	2.7E+00	1.2E+02	2.1E−09	1.5E−08	1.2E−04	1.0E−05	3.2E−04
	3.0	4.1E+06	9.0E+05	3.7E+01	3.2E+02	2.5E−06	4.9E−06	2.0E−03	1.1E−03	1.1E−02
	4.0	4.3E+06	6.6E+06	1.7E+03	1.2E+03	1.8E−02	1.2E−02	7.9E−02	4.2E−01	1.5E+00
	5.0	4.4E+06	2.6E+07	2.3E+04	3.0E+03	3.4E+00	1.9E+00	7.8E−01	1.6E+01	3.8E+01
	7.0	3.9E+06	1.3E+08	5.9E+05	9.5E+03	1.3E+03	7.5E+02	1.1E+01	1.1E+03	2.5E+03
	10.0	2.7E+06	3.7E+08	6.5E+06	2.2E+04	1.0E+05	6.1E+04	1.2E+02	3.6E+04	8.1E+04
^{55}Co	0.1	6.3E+05	7.5E+07	8.3E−04						
	0.3	1.0E+06	1.3E+08	4.6E−03	1.5E−09					
	0.5	1.5E+06	1.9E+08	1.7E−02	6.5E−06	6.7E−87			3.7E−76	
	1.0	2.3E+06	2.8E+08	1.8E−01	3.5E−02	3.8E−40	3.4E−18	8.9E−15	1.5E−35	3.1E−14
	1.5	2.8E+06	3.4E+08	1.4E+00	1.3E+00	2.1E−24	4.2E−12	2.0E−10	7.0E−22	1.9E−09
	2.0	3.1E+06	3.8E+08	9.7E+00	1.0E+01	1.6E−16	1.6E−08	8.2E−08	5.7E−15	1.7E−06
	2.5	3.3E+06	4.3E+08	5.6E+01	4.0E+01	8.8E−12	4.3E−06	4.3E−06	8.7E−11	1.9E−04
	3.0	3.4E+06	4.7E+08	3.0E+02	1.1E+02	1.2E−08	2.8E−04	7.3E−05	5.8E−08	6.9E−03
	4.0	3.6E+06	5.4E+08	6.4E+03	4.1E+02	1.0E−04	9.7E−02	3.2E−03	2.4E−04	1.1E+00
	5.0	3.8E+06	6.2E+08	6.6E+04	1.0E+03	2.2E−02	5.2E+00	4.0E−02	4.4E−02	3.2E+01
	7.0	3.8E+06	7.8E+08	1.5E+06	3.3E+03	9.5E+00	8.3E+02	1.1E+00	2.7E+01	2.3E+03
	10.0	3.2E+06	1.0E+09	1.7E+07	8.1E+03	7.5E+02	4.6E+04	1.9E+01	4.6E+03	8.1E+04
^{56}Ni	0.1	7.5E+05	1.0E+07	7.7E−02						
	0.3	6.0E+05	1.3E+07	2.0E−02						3.9E−58
	0.5	6.8E+05	2.3E+07	2.0E−02						6.5E−37
	1.0	8.7E+05	5.1E+07	9.8E−01				1.0E−14	2.1E−55	6.7E−19
	1.5	1.0E+06	8.2E+07	8.5E+00				6.7E−10	1.0E−34	7.3E−12
	2.0	1.1E+06	1.1E+08	4.3E+01				6.1E−07	2.6E−24	5.9E−08
	2.5	1.1E+06	1.5E+08	1.8E+02				6.4E−05	4.7E−18	2.0E−05
	3.0	1.2E+06	1.8E+08	6.7E+02				1.9E−03	7.4E−14	1.3E−03
	4.0	1.2E+06	2.5E+08	7.2E+03				1.8E−01	1.5E−08	3.5E−01
	5.0	1.2E+06	3.3E+08	4.9E+04				3.3E+00	2.6E−05	1.3E+01
	7.0	1.2E+06	5.4E+08	8.1E+05				1.1E+02	1.9E−01	1.3E+03
	10.0	8.0E+05	1.1E+09	9.0E+06				1.2E+03	1.7E+02	5.6E+04

proton- or neutron-induced reactions dominate by many orders of magnitude, but the disagreement casts doubt over the reliability of calculated α-particle reaction rates under conditions where these reactions are competing strongly.

Disagreements by factors > 3 with proton- or neutron-induced reactions are limited to reactions with $N = 28$ compound nuclei or reactions for which an alternative exit channel is dominant.

Table 2 contains calculated rates for numerous reactions for which experiment-based rates already exist and which naturally take precedence. The experimental cross sections were the basis for our optical-model parameter specifications and the calculated rates are presented in such cases simply for the sake of completeness.

References

Becchetti, F. P., and Greenlees, G. W. (1969). *Phys. Rev.* **182**, 1190.

Bodansky, D., Clayton, D. D., and Fowler, W. A. (1968). *Astrophys. J. Suppl.* No. 148, **16**, 299.

Fowler, W. A., Caughlan, G. R., and Zimmerman, B. A. (1967). *Ann. Rev. Astron. Astrophys.* **5**, 525.

Hansper, V. Y., Morton, A. J., Tims, S. G., Tingwell, C. I. W., Scott, A. F., and Sargood, D. G. (1993). *Nucl. Phys.* A **551**, 158.

Hoffman, R. D., and Woosley, S. E. (1992). Tables of reaction rates for nucleosynthesis for charged particle, weak, and neutrino interactions ($Z \leq 44$): version 92.1, University of California, Santa Cruz, unpublished.

Howard, M. W., Arnett, W. D., Clayton, D. D., and Woosley, S. E. (1972). *Astrophys. J.* **175**, 201.

McFadden, L., and Satchler, R. (1966). *Nucl. Phys.* **84**, 177.

Mann, F. M. (1976). HAUSER*4, a computer code to calculate nuclear cross sections, Hanford Engineering and Development Laboratory report HEDL-TME 76–80, unpublished.

Morton, A. J., Scott, A. F., Tims, S. G., Hansper, V. Y., and Sargood, D. G. (1994). *Nucl. Phys.* A **573**, 276.

Scott, A. F., Morton, A. J., Tingwell, C. I. W., Tims, S. G., Hansper, V. Y., and Sargood, D. G. (1991). *Nucl. Phys.* A **523**, 373.

Solomon, S. B., and Sargood, D. G. (1978). *Astrophys. J.* **223**, 697.

Tepel, J. W., Hofmann, H. M., and Weidenmüller, H. A. (1974). *Phys. Lett.* B **49**, 1.

Tims, S. G., Tingwell, C. I. W., Hansper, V. Y., Scott, A. F., and Sargood, D. G. (1988). *Nucl. Phys.* A **483**, 354.

Tims, S. G., Scott, A. F., Morton, A. J., Hansper, V. Y., and Sargood, D. G. (1993). *Nucl. Phys.* A **563**, 473.

Tingwell, C. I. W., Hansper, V. Y., Tims, S. G., Scott, A. F., Morton, A. J., and Sargood, D. G., (1989). *Nucl. Phys.* A **496**, 127.

Ward, R. A., and Fowler, W. A. (1980). *Astrophys. J.* **238**, 266.

Woosley, S. E., Arnett, W. D., and Clayton, D. D. (1973). *Astrophys. J. Suppl.* No. 231, **26**, 231.

Woosley, S. E., Fowler, W. A., Holmes, J. A., and Zimmerman, B. A. (1975). Tables of thermonuclear reaction rate data for intermediate mass nuclei, Caltech preprint OAP-422, unpublished.

Woosley, S. E., Fowler, W. A., Holmes, J. A., and Zimmerman, B. A. (1978). *At. Data Nucl. Data Tables* **22**, 371.

Manuscript received 5 September, accepted 19 October 1994